Published in final edited form as:
Ann Biomed Eng. 2013 January ; 41(1): . doi:10.1007/s10439-012-0630-4.

Cationic Nanoparticles Have Superior Transvascular Flux into Solid Tumors: Insights from a Mathematical Model

Triantafyllos Stylianopoulos[1], **Konstantinos Soteriou**[1], **Dai Fukumura**[2], and **Rakesh K. Jain**[2]

[1]Department of Mechanical and Manufacturing Engineering, University of Cyprus, 1678 Nicosia, Cyprus

[2]Edwin L. Steele Laboratory for Tumor Biology, Massachusetts General Hospital, Harvard Medical School, Boston, MA 02114, USA

Abstract

Despite their great promise, only a few nanoparticle formulations have been approved for clinical use in oncology. The failure of nano-scale drugs to enhance cancer therapy is in large part due to inefficient delivery. To overcome this outstanding problem, a better understanding of how the physical properties (i.e., size, surface chemistry, and shape) of nanoparticles affect their transvascular transport in tumors is required. In this study, we developed a mathematical model for nanoparticle delivery to solid tumors taking into account electrostatic interactions between the particles and the negatively-charged pores of the vessel wall. The model predictions suggest that electrostatic repulsion has a minor effect on the transvascular transport of nanoparticles. On the contrary, electrostatic attraction, caused even by small cationic charges (surface charge density less than 3×10^{-3} C/m^2) can lead to a twofold or more increase in the transvascular flux of nanoparticles into the tumor interstitial space. Importantly, for every nanoparticle size, there is a value of charge density above which a steep increase in transvascular transport is predicted. Our model provides important guidelines for the optimal design of nanoparticle formulation for delivery to solid tumors.

Keywords

Vascular permeability; Electrostatic and hydrodynamic interactions; Surface charge density; Nanomedicine; Cancer therapy

Address correspondence to Triantafyllos Stylianopoulos, Department of Mechanical and Manufacturing Engineering, University of Cyprus, 1678 Nicosia, Cyprus and Rakesh K. Jain, Edwin L. Steele Laboratory for Tumor Biology, Massachusetts General Hospital, Harvard Medical School, Boston, MA 02114, USA. tstylian@ucy.ac.cy, jain@steele.mgh.harvard.edu.

Associate Editor Konstantinos Konstantopoulos oversaw the review of this article.

ELECTRONIC SUPPLEMENTARY MATERIAL
The online version of this article (doi:10.1007/s10439-012-0630-4) contains supplementary material, which is available to authorized users.

CONFLICT OF INTEREST

R.K.J. received research grants from Dyax, Med-Immune and Roche; consultant fees from Dyax, Enlight, Noxxon and SynDevRx; owns equity in Enlight, SynDevRx and XTuit, serves on the Board of Directors of XTuit and Board of Trustees of H&Q Capital Management. No reagents or funding from these companies was used in these studies. Therefore, there is no significant financial or other competing interest in the work. The other authors declare no competing financial interests.

INTRODUCTION

Nanomedicine is a promising modality for cancer detection and treatment.[22,40] Advances in nanotechnology have led to the development of nanoparticles whose size, surface chemistry and shape can be easily controlled.[6,29,36] However, only a few nanoparticle formulations have been approved to date for clinical use in oncology.[22] Although the enhanced permeability and retention (EPR) effect has served as a key rationale for the use of nano-scale drugs to treat solid tumors, physiological barriers posed by the tumor microenvironment hinder homogeneous delivery of nanoparticles in amounts sufficient to eradicate cancer. [7,22] Therefore, we need to better understand these barriers and develop criteria for the optimal design of nanoparticles.

Many experimental studies have investigated the effect of particle size on transvascular and interstitial transport in solid tumors.[8,9,14,25,26,28,43] These studies have shown a drop in the transport properties of the particles once their size approaches the pore size of the vascular wall or the interstitial space. On the contrary, there is limited work on how the surface charge of the particles affects transvascular flux. Experimental findings have shown that cationic nanoparticles preferentially extravasate from tumor vessels, presumably due to electrostatic interactions with the negatively-charged glycocalyx of vascular endothelial cells.[5,12,32] However, the parameters affecting transvascular transport such as the size and surface charge density of the nanoparticles and the pores of the vessel wall have not been analyzed rigorously.

In previous research, we developed a mathematical framework for the transvascular transport of nanomedicines taking into account steric and hydrodynamic interactions between the particles and the pores of the vessel wall.[8] The current paper extends our framework by incorporating the surface charge of the nanoparticles and the resulting electrostatic interactions. We used an existing algorithm for modeling tumor-induced angiogenesis to generate the vascular network in this study.[24,42] The vasculature consists of two inlets and two outlets (Fig. 1) and the pores of the vessel wall are taken by a unimodal distribution based on our previous work.[15,16] The model accounts for the size and surface charge density of both the particles and the pores of the vessel wall. To account for steric and hydrodynamic interactions, a theory developed by Bungay and Brenner[4] was employed, while electrostatic interactions were calculated based on a methodology developed by Smith and Deen.[34]

MATERIALS AND METHODS

Formulation of the Mathematical Model

We employed an existing algorithm that simulates the process of tumor-induced angiogenesis based on the gradients of vascular endothelial growth factors and fibronectin.[24,42] The vascular domain consists of two parent vessels, from which neoplastic blood vessels are extending towards the tumor[42] (Fig. 1).

The mathematical model requires coupling of fluid flow and nanoparticle transport in the vascular and interstitial spaces.

Coupling of Fluid Flow

Blood volumetric flow rate in a vessel (Q_{vascular}) is assumed to be axial and follows Poiseuille's law,

$$Q_{\text{vascular}} = -\frac{\pi d^4}{128\mu}\frac{\Delta p_{\text{v}}}{\Delta x}, \quad (1)$$

where d is the vessel diameter, Δp_{v} is the vascular pressure difference that corresponds to a vascular length Δx and μ is the blood viscosity.

Volumetric fluid flow rate across the vessel wall ($Q_{\text{transvascular}}$) follows Starling's law,[2]

$$Q_{\text{transvascular}} = L_p S(p_{\text{v}} - p_{\text{i}}), \quad (2)$$

where L_p is the hydraulic conductivity of the vessel wall, S is the surface area of the vessel and p_{i} is the interstitial fluid pressure. Notice that in Eq. (2) we neglect osmotic pressures since in solid tumors they have a negligible effect to fluid flow across the vessel wall.[1,35,39]

Interstitial volumetric fluid flow rate (Q_{tissue}) follows Darcy's law,[2,37]

$$Q_{\text{tissue}} = -K_t A_{\text{C}}\frac{\Delta p_{\text{i}}}{\Delta x}, \quad (3)$$

where K_t is the hydraulic conductivity of the interstitial space, Δp_{i} is the interstitial pressure difference that corresponds to a tissue length Δx, and A_{C} is the tissue cross-sectional area. The tissue cross-sectional area is related to the vascular density, S_{v}, and the diameter of the vessel, d, by $A_{\text{C}} = \pi d/S_{\text{v}}$.[1]

Coupling of Nanoparticle Transport

Coupling of nanoparticle transport between the vascular and interstitial spaces is based on the following assumptions.

Inside the blood vessels diffusion is negligible and the mass balance takes the form:

$$\frac{dc_{\text{v}}}{dt} = -v\frac{\Delta c_{\text{v}}}{\Delta x}, \quad (4)$$

where v is the fluid velocity which is determined by dividing Q_{vascular} in Eq. (1) by the cross-sectional area of the vessel, c_{v} is the intravascular concentration of the nanoparticle and Δc_{v} is the concentration difference that corresponds to a vascular length Δx.

In the interstitial space transport of nanoparticles is governed by the convection–diffusion equation,[2]

$$\frac{dc_{\text{i}}}{dt} + v_{\text{i}}\nabla c_{\text{i}} = D\nabla^2 c_{\text{i}}, \quad (5)$$

where c_{i} is the concentration of the nanoparticle in the interstitial space, D is the diffusion coefficient, and v_{i} is the interstitial fluid velocity which is calculating by dividing Q_{tissue} in Eq. (3) by A_{C}.

Transport across the tumor vessel wall, φ, is given by Starling's approximation as[2]

$$\phi = L_p S (p_v - p_i)(1-\sigma)\frac{c_v e^{P_e} - c_i}{e^{P_e}-1} \quad \text{with} \quad P_e = L_p(1-\sigma)\frac{(p_v - p_i)}{P}, \quad (6)$$

where *Pe* is the Péclet number across the vessel wall, and *P* is the vascular permeability of the nanoparticle through the pores of the wall. Using theory for transport of particles through cylindrical pores[11] we calculate the hydraulic conductivity, L_p, vascular permeability, *P*, and reflection coefficient, σ, by the equations:

$$L_p = \frac{\gamma r_o^2}{8\mu L}, \quad P = \frac{\gamma H D_o}{L}, \quad \sigma = 1 - W, \quad (7)$$

where γ is the fraction of vessel wall surface area occupied by pores, r_o is the pore radius, *L* is the thickness of the vessel wall, and D_o is the diffusion coefficient of the particle in free solution at 37 °C.

The parameters *H* and *W* account for hydrodynamic and electrostatic interactions and for dilute solutions are given by the equations[11]:

$$H = 2\int_0^{1-\lambda} K^{-1} e^{-E/kT} \beta d\beta, \quad (8)$$

$$W = 4\int_0^{1-\lambda} G(1-\beta^2) e^{-E/kT} \beta d\beta, \quad (9)$$

where λ is the ratio of the particle size over the pore size, *E* is the electrostatic energy of interaction between the nanoparticle and the pore, *k* is the Boltzmann's constant, *T* is the absolute temperature, $K(\lambda,\beta)$ and $G(\lambda,\beta)$ are hydrodynamic functions, and β is the radial distance in the pore divided by the pore radius (i.e., r/r_o in Supplementary Fig. 1).

To calculate the hydrodynamic functions, $K(\lambda,\beta)$ and $G(\lambda,\beta)$, the centerline approximation is employed, which suggests that use of the centerline values, $K(\lambda,0)$ and $G(\lambda,0)$ leads to reasonably accurate estimates of *H* and *W*.[11] Therefore, Eqs. (8) and (9) are written as:

$$H = 2K^{-1}(\lambda,0)\int_0^{1-\lambda} e^{-E/kT} \beta d\beta, \quad (10)$$

$$W = 4G(\lambda,0)\int_0^{1-\lambda} (1-\beta^2) e^{-E/kT} \beta d\beta. \quad (11)$$

Analytical expressions of the hydrodynamic coefficients $K(\lambda,0)$ and $G(\lambda,0)$ are given by Bungay and Brenner.[4,11] These expressions are composites of asymptotic centerline results for small and for closely fitting spheres, are valid for $0 \le \lambda < 1$ and are accurate to within 10% for all values of λ. Notice that in the absence of electrostatic interactions (i.e., $E = 0$), Eqs. (10) and (11) are written as $H = \Phi K^{-1}(\lambda,0)$ and $W = \Phi(2 - \Phi)G(\lambda,0)$, where Φ is the partition coefficient (for $E = 0$, $\Phi = (1 - \lambda)^2$).

Calculation of Electrostatic Energy

To calculate the electrostatic energy between the nanoparticle and each pore of the vessel wall a methodology developed by Smith and Deen[34] is used. This methodology employs the

linear form of the Poisson–Boltzmann equation to provide theoretical results for the electrostatic double-layer interaction between a particle and a cylindrical pore. The particle is assumed to be solid and spherical with a given surface charge density. Analytical expressions of the electrostatic energy are calculated based on the ratio of particle size to pore size λ, the ionic strength, and the surface charge density of the particle and the cylindrical pore. The theory accounts for both electrostatic attraction and repulsion.

The electrostatic energy, E, between the pore and the solid sphere is related to the free energy, ΔG by

$$E=r_o\varepsilon\left(\frac{RT}{F}\right)^2\Delta G, \quad (12)$$

where R is the gas constant, T is the absolute temperature, ε the permittivity, and r_o the radius of the pore. The free energy, ΔG, is given by

$$\Delta G=G_{\mathrm{sp}}-G_{\mathrm{s}}-G_{\mathrm{p}}, \quad (13)$$

where G_{sp} is the energy of interaction between the sphere and the cylindrical pore, G_{s} the energy of the sphere and G_{p} the energy of the pore.

Assuming solid spheres of constant surface charge, q, and employing the linearized Poisson–Boltzmann equation, the free energy is given by the surface integral of the electric potential, Ψ, as

$$G=\frac{q}{2}\int\Psi(q)dA, \quad (14)$$

where A denotes the area of the surface.

Finally, the electric potential is calculated by the solution of the linearized Poisson–Boltzmann equation:

$$\nabla^2\Psi=\tau^2\Psi \quad (15)$$

which is valid for the space inside the pore and τ is the inverse of the Debye length. Whereas, inside the spherical particle and inside the solid material surrounding the pore, the electric potential is described by the Laplace's equation (Supplementary Fig. 1).

The calculation of the free energy, ΔG, is given by the solution of Eqs. (13)–(15). This system of equations has an analytical solution given in the reference (Smith and Deen,[34] Eq. 29) and was employed in the current study.

Solution Strategy

We first solve the steady-state fluid problem (Eqs. 1–3) and calculate the pressure distribution in the vascular and interstitial spaces. The vascular and interstitial spaces are discretized by nodes as shown in Supplementary Fig. 2. Each node belonging to the vascular space is assigned a pore diameter taken randomly by a unimodal distribution with a given mean and standard deviation. Therefore, each of the "vascular" nodes has its own values of L_p, P, and σ (Eq. 7). Conservation of the fluid requires that at each node the volume of fluid entering the node is the same as the fluid exiting the node, i.e., $\Sigma_i\, Q_i = 0$ for each node i. As

for boundary conditions, the vascular pressure at the inlets and outlets of the network is presubscribed. The normal tissue surrounding the tumor is assumed to have functional lymphatic vessels and thus the fluid pressure there is set to zero (Fig. 1).

Subsequently, we solve the transient transport problem to calculate the concentration of the nanoparticles (Eqs. 4–6). The transient nanoparticle transport problem is solved with a finite difference scheme. Central differencing for diffusion, upwind differencing for convection and a fourth-order Runge–Kutta for time integration were used. For boundary conditions, the concentration of the particles at the inlets is specified and decays exponentially with a time constant equal to the blood half-life of the particle. In addition, the concentration at the outlets and at the boundary of the interstitial space is set to zero (Fig. 1).

Calculation of Transvascular Flux

The transvascular flux or effective vascular permeability, P_{eff}, is calculated in a region at the center of the tumor by recording the average concentration of nanoparticles in this region through time and fitting to these data the following equation[8]:

$$\frac{C}{C_o}=\frac{P_{\text{eff}}S_{\text{v}}K_{\text{d}}}{1-P_{\text{eff}}S_{\text{v}}K_{\text{d}}}\left(e^{-P_{\text{eff}}S_{\text{v}}t}-e^{-t/K_{\text{d}}}\right). \quad (16)$$

where C is the average concentration in the region of interest, C_o is the initial concentration of the particles and K_{d} is the time constant of concentration decrease in the plasma related to the clearance time.

Supplementary Fig. 3 shows how Eq. (16) fits with the model predictions of the averaged concentration.

Model Parameters

Nanoparticles might vary considerably in both size and surface charge. In this study, particles with diameters in the range of 6–200 nm were considered, which is the range of size for current nanomedicines. [8,29] The surface charge density $|q_{\text{s}}|$ of the particles ranged from 0.0 to 0.10 C/m^2, based on values for gold nanoparticles and consistent with pertinent studies. [27,36] The interstitial diffusivities of the nanoparticles, D, and the time constant of concentration decay, K_{d}, depend on the size and the surface chemistry of the nanoparticles and were determined based on our experimental measurements.[25,28,29]

The size of the pores in the tumor vessel wall depends on the tumor type and the site of growth. Brain tumor xenografts (U87 glioblastoma) have pore cut-off sizes ranging from 7 to 100 nm, while other cancer cell lines (LS174T, Shionogi, HCaI, ST-12, ST-8) when implanted subcutaneously in mice have a maximum pore cut-off size from 380 to 780 nm in diameter.[16] In previous research, we found that when a unimodal distribution with mean pore size of 400 nm and a standard deviation of 60 nm was used, the model provided very accurate predictions for the transvascular flux of particles 12, 60, and 120 nm in diameter in two leaky tumor models.[8] Therefore, we used these values here. Tumor vessels are negatively-charged due to vascular glycocalyx.[31] Lacking information of the charge of the vessel wall, we assumed a surface charge density of −0.05 C/m^2 based on other studies.[34] Except where noted otherwise, the physiological ionic strength of 0.15 M was used, which results in a Debye length in the order of 1 nm. The size of the computational domain was 2 cm for a 1 cm diameter tumor, the blood viscosity was 3×10^{-5} mmHg s, the vascular pressure at the inlets and outlets was 25 and 5 mmHg, respectively, the vascular density S_{v} was set to 100 cm^{-1}, the vessel wall thickness, L, was 5 μm, the vessel diameter was taken to be 15 μm and the conductivity of the interstitial space (normal and tumor) was 8×10^{-7} cm^2/mmHg s (Table 1).

In previous research, we showed that using these parameters our mathematical model predicted successfully the transvascular flux of neutral nanoparticles of diameters 12, 60, and 120 nm in two different transplanted tumor models.[8] The interstitial fluid pressure as well as the pressure difference between the vascular and interstitial space (transvascular pressure difference) are shown in Fig. 2. Interstitial fluid pressure is elevated at the center of the tumor, resulting in negligible pressure gradients across the vessel wall. The effect of pore size on transvascular pressure difference is shown in Supplementary Fig. 4.

RESULTS

Electrostatic Repulsion is Important for Pore Diameters Comparable to the Debye Length

Electrostatic repulsion decreases the hydrodynamic coefficients H and W (Eqs. 8 and 9), which in turn reduce the vascular permeability, P, and reflection coefficient, σ (Eq. 7) and thus, the transvascular flux of nanoparticles (Eq. 6). In tumors, the pores of the vessel wall can vary from a few nanometers to hundreds of nanometers depending on the tumor type and location. Therefore, in Fig. 3, we plot H and W as a function of the particle surface charge density and for pore diameters, d_p, ranging from 20 to 300 nm. The ratio of the particle size to pore size, λ, was kept constant at 0.3, and only negatively-charged particles were considered. The figure shows that electrostatic repulsion affects significantly the coefficients H and W for small pore diameters, while the effect is less important for large pores. The range of electrostatic interactions is determined by the Debye length. For our simulations the Debye length was chosen as ~1 nm. When the Debye length is comparable to the diameter of the pores, electrostatic forces are strong because the electrostatic double layers of the pore and the particle are close to each other. As the pore size increases the double layers separate and only particles that are close to the wall of the cylindrical pore will interact.

Ionic Strength Significantly Affects the Transvascular Flux of Nanoparticles

As the ionic strength increases, the Debye length decreases and the electrostatic interactions diminish. Figure 4a shows the transvascular flux of negatively-charged particles of four different sizes (λ = 0.1, 0.2, 0.3, and 0.5) as a function of the ionic strength. The surface charge of the particles is −0.05 C/m^2, and the mean pore size is 400 nm with a standard deviation of 60 nm. Low ionic strength causes a steep decrease in the flux of the particles independently of their size. Figure 4b presents the transvascular flux as a function of particle surface charge density and for four values of the ionic strength (C = 0.005, 0.01, 0.06, and 0.15 M). The pore distribution is the same as in Fig. 4a. The transvascular flux of the negatively-charged particles decreases as their charge increases. For physiological values of the ionic strength (0.15 M), however, the effect of repulsive interactions on the transport of the particles is not significant, which suggests a minimal excluded volume effect. Furthermore, neutral particles at low ionic strength exhibit a lower flux because even if they do not carry a charge, the interaction potential with the charged pores is not zero.

Cationic Charge is Optimal for Nanoparticle Transvascular Flux

Figure 5a shows the transvascular flux of negatively-charged particles as a function of the particle's surface charge density and when the ratio of the particle size to pore size, λ, is 0.1, 0.3, and 0.5. The mean pore size is 400 nm with a standard deviation of 60 nm. For neutral particles the flux decreases with the particle size as a result of steric and hydrodynamic interactions. For negatively-charged particles, electrostatic repulsion causes a slight and uniform decrease in the extravasation rate of the particles. More significant is the effect of charge on the transvascular transport for positively-charged nanoparticles. Figure 5b shows the effect of electrostatic attraction on the extravasation of nanoparticles. The transvascular flux is plotted as a function of the surface charge density and for three different sizes of

particles, $\lambda = 0.1$, 0.3, and 0.5. Even relatively small positive surface charges can cause an up to threefold increase in the particle flux across the vessel wall. The effect of electrostatic attraction becomes more important for larger particles as the forces become stronger.

Figure 6 depicts the transvascular flux of nanoparticles 10, 60, and 120 nm in diameter as a function of the mean pore size and varying the surface charge density (positively-charged, neutral and negatively-charged). There is an ideal pore size for the particles that transvascular flux reaches a maximum. At smaller pores, steric, hydrodynamic and electrostatic interactions between the particles and the pores hinder extravasation but transport is maintained due to a pressure gradient across the vessel wall (convection). At larger pores, these interactions diminish which enhances transport, but the transvascular pressure gradient disappears (Supplementary Fig. 4) rendering diffusion as the only transport mechanism. Therefore, there is an optimum pore size where both convection and diffusion contribute to the extravasation of the particles. Electrostatic interactions are significant for smaller pores, while they have no effect as the mean pore size passes a value. This value depends on the size of the particle and the surface charge density. A positive surface charge can significantly increase the flux of nanoparticles and switch the optimal flux to smaller pore sizes.

DISCUSSION

Nanomedicine is an emerging and promising approach for the treatment of cancer. Nanoparticle formulations might be advantageous over conventional chemotherapeutics because they can incorporate multiple diagnostic and/or therapeutic agents, and can preferentially accumulate in tumors due to the EPR effect and the incorporation of specific targeting moiety. The relatively large size of nano-scale drugs, however, might inhibit their homogeneous distribution within solid tumors and thus, compromise the therapeutic outcome. Research for the optimization of nanoparticle delivery to date has been mainly focused on modifying the tumor microenvironment *via* vascular or interstitial normalization[8,13,20,21] or the use of targeting ligands.[17,30,38] A better design of nanoparticles (i.e., optimal size, charge, and shape) could also overcome the transport barriers and further improve intratumoral penetration.[10,41]

Many components of the tumor micro-environment have an electric charge. The vascular glycocalyx renders the blood vessels negatively-charged, while in the interstitial space the hyaluronic acid consists of highly anionic molecules and the collagen fibers have a slightly positive charge.[31,36] Therefore, electrostatic interactions between nanoparticles and components of the tumor micro-environment could play an important role on drug delivery. In this paper, we developed a mathematical model to study how the surface charge of nanoparticles can affect transport across the tumor vessel wall. The model predicted that transvascular transport of negatively-charged particles is hindered only when the pore size is comparable to the Debye length. Of note, for pores of the tumor vessel wall, whose size is on the order of hundreds of nanometers, the effect of electrostatic repulsion must be negligible (Figs. 3 and 6). On the contrary, electrostatic attraction, caused by positively-charged particles, can significantly increase transvascular flux (Figs. 5b and 6). Electrostatic attraction, which enhances transvascular transport, competes steric and hydrodynamic interactions, which hinder transport. As a result, it seems that for every nanoparticle size, there is a value of surface charge density above which electrostatic forces become dominant and a steep increase in transvascular flux is predicted (Fig. 5b). In addition, for smaller pore sizes (<100 nm in Fig. 6a) steric and hydrodynamic forces must dominate and for that reason we do not see important effects of charge on the transvascular transport of nanoparticles. As the pore size increases the effect of electrostatic interactions should become dominant and an increase in transport is predicted. Finally, when vascular pores are

getting very large (>300 nm in Fig. 6a) compared to the size of the particles all three types of interactions diminish and the effect of charge disappears. Given the fact that some tumor types, such as brain and pancreatic cancers, have relatively small vascular pores, while in other tumors, such as breast cancers, the pore size might exceed 1 μm in diameter,[16] the advantage of cationic nanoparticles should depend on the tumor type.

The model predictions are in agreement with the experimental findings that the transvascular flux of cationic molecules is higher than that of their neutral or anionic counterparts.[12] Also experiments have shown that cationic liposomes selectively accumulate in tumor vessels, presumably due to electrostatic attraction, and improve intratumoral delivery of encapsulated chemotherapeutics.[5,32] On the other hand, neutral particles have been shown to diffuse faster than the charged ones in the interstitial space of tumors and thus, improve intratumoral penetration.[36] Therefore, particles with initial positive surface charge that switches to neutral once they enter the tumor interstitial space would be the ideal design as far as transport is concerned.[41] High positive charges, however, might affect plasma clearance rates and reduce the circulation time of the particles.[23]

The tumor micro-environment is too complex to be precisely represented by a single mathematical model. Therefore a number of assumptions had to be made. Our model is limited in that it does not account for the three-dimensional structure of the vasculature. In addition, it assumes a uniform vessel diameter and blood viscosity. However, the diameter of tumor vessels is not uniform[45] and the plasma leakage through the pores of the vessels increases the concentration of red blood cells (hemoconcentration) which might alter the viscosity value.[33] Another limitation of the model is that the expressions for the hindrance coefficients H and W (Eqs. 8 and 9) are valid for only dilute solutions. Positive surface charges larger than these employed in the current study might render the dilute solution theory invalid and the predictions of the model might become unrealistic.[34]

To our knowledge this is the first model for the delivery of nanoparticles to solid tumors that takes into account steric, hydrodynamic and electrostatic interactions between the particles and the pores of the vessel wall. Furthermore, while we employed here a computer generated vascular network, our methodology is general and can be directly applied to vascular networks of any geometry.

Supplementary Material

Refer to Web version on PubMed Central for supplementary material.

Acknowledgments

The authors thank Dr. Vikash Chauhan for his insightful comments on the manuscript. This work was supported by a Marie-Curie International Reintegration Grant (No. PIRG08-GA-2010-276894), the National Cancer Institute (P01-CA080124, R01-CA126642, R01-CA115767, R01-CA096915, R01-CA085140, R01-CA098706, T32-CA073479, Federal Share Proton Beam Program Income Grant), and a DoD Breast Cancer Research Innovator award (W81XWH-10-1-0016).

References

1. Baish JW, Netti PA, Jain RK. Transmural coupling of fluid flow in microcirculatory network and interstitium in tumors. Microvasc Res. 1997; 53:128–141. [PubMed: 9143544]
2. Baxter LT, Jain RK. Transport of fluid and macromolecules in tumors. II. Role of heterogeneous perfusion and lymphatics. Microvasc Res. 1990; 40:246–263. [PubMed: 2250603]
3. Boucher Y, Jain RK. Microvascular pressure is the principal driving force for interstitial hypertension in solid tumors: implications for vascular collapse. Cancer Res. 1992; 52:5110–5114. [PubMed: 1516068]

4. Bungay PM, Brenner H. The motion of a closely fitting sphere in a fluid-filled tube. Int J Multiph Flow. 1973; 1:25–56.
5. Campbell RB, Fukumura D, Brown EB, Mazzola LM, Izumi Y, Jain RK, Torchilin VP, Munn LL. Cationic charge determines the distribution of liposomes between the vascular and extravascular compartments of tumors. Cancer Res. 2002; 62:6831–6836. [PubMed: 12460895]
6. Chauhan VP, Popovic Z, Chen O, Cui J, Fukumura D, Bawendi MG, Jain RK. Fluorescent nanorods and nanospheres for real-time in vivo probing of nanoparticle shape-dependent tumor penetration. Angew Chem Int Ed Engl. 2011; 50:11417–11420. [PubMed: 22113800]
7. Chauhan VP, Stylianopoulos T, Boucher Y, Jain RK. Delivery of molecular and nanomedicine to tumors: transport barriers and strategies. Annu Rev Chem Biomol Eng. 2011; 2:281–298. [PubMed: 22432620]
8. Chauhan VP, Stylianopoulos T, Martin JD, Popovic Z, Chen O, Kamoun WS, Bawendi MG, Fukumura D, Jain RK. Normalization of tumour blood vessels improves the delivery of nanomedicines in a size-dependent manner. Nat Nanotechnol. 2012; 7:383–388. [PubMed: 22484912]
9. Clauss MA, Jain RK. Interstitial transport of rabbit and sheep antibodies in normal and neoplastic tissues. Cancer Res. 1990; 50:3487–3492. [PubMed: 2340499]
10. Decuzzi P, Ferrari M. Design maps for nanoparticles targeting the diseased microvasculature. Biomaterials. 2008; 29:377–384. [PubMed: 17936897]
11. Deen WM. Hindered transport of large molecules in liquid-filled pores. AIChE J. 1987; 33:1409–1425.
12. Dellian M, Yuan F, Trubetskoy VS, Torchilin VP, Jain RK. Vascular permeability in a human tumour xenograft: molecular charge dependence. Br J Cancer. 2000; 82:1513–1518. [PubMed: 10789717]
13. Diop-Frimpong B V, Chauhan P, Krane S, Boucher Y, Jain RK. Losartan inhibits collagen I synthesis and improves the distribution and efficacy of nanotherapeutics in tumors. Proc Natl Acad Sci USA. 2011; 108:2909–2914. [PubMed: 21282607]
14. Gerlowski LE, Jain RK. Microvascular permeability of normal and neoplastic tissues. Microvasc Res. 1986; 31:288–305. [PubMed: 2423854]
15. Hashizume H, Baluk P, Morikawa S, McLean JW, Thurston G, Roberge S, Jain RK, McDonald DM. Openings between defective endothelial cells explain tumor vessel leakiness. Am J Pathol. 2000; 156:1363–1380. [PubMed: 10751361]
16. Hobbs SK, Monsky WL, Yuan F, Roberts WG, Griffith L, Torchilin VP, Jain RK. Regulation of transport pathways in tumor vessels: role of tumor type and microenvironment. Proc Natl Acad Sci USA. 1998; 95:4607–4612. [PubMed: 9539785]
17. Hood JD, Bednarski M, Frausto R, Guccione S, Reisfeld RA, Xiang R, Cheresh DA. Tumor regression by targeted gene delivery to the neovasculature. Science. 2002; 296:2404–2407. [PubMed: 12089446]
18. Jain RK. Transport of molecules across tumor vasculature. Cancer Metastasis Rev. 1987; 6:559–593. [PubMed: 3327633]
19. Jain RK. Determinants of tumor blood flow: a review. Cancer Res. 1988; 48:2641–2658. [PubMed: 3282647]
20. Jain RK. Normalizing tumor vasculature with antiangiogenic therapy: a new paradigm for combination therapy. Nat Med. 2001; 7:987–989. [PubMed: 11533692]
21. Jain RK. Normalization of tumor vasculature: an emerging concept in antiangiogenic therapy. Science. 2005; 307:58–62. [PubMed: 15637262]
22. Jain RK, Stylianopoulos T. Delivering nanomedicine to solid tumors. Nat Rev Clin Oncol. 2010; 7:653–664. [PubMed: 20838415]
23. Longmire M, Choyke PL, Kobayashi H. Clearance properties of nano-sized particles and molecules as imaging agents: considerations and caveats. Nanomedicine (Lond). 2008; 3:703–717. [PubMed: 18817471]
24. McDougall SR, Anderson AR, Chaplain MA. Mathematical modelling of dynamic adaptive tumour-induced angiogenesis: clinical implications and therapeutic targeting strategies. J Theor Biol. 2006; 241:564–589. [PubMed: 16487543]

25. Netti PA, Berk DA, Swartz MA, Grodzinsky AJ, Jain RK. Role of extracellular matrix assembly in interstitial transport in solid tumors. Cancer Res. 2000; 60:2497– 2503. [PubMed: 10811131]
26. Nugent LJ, Jain RK. Extravascular diffusion in normal and neoplastic tissues. Cancer Res. 1984; 44:238–244. [PubMed: 6197161]
27. Park S, Hamad-Schifferli K. Evaluation of hydrodynamic size and zeta-potential of surface-modified Au nanoparticle-DNA conjugates via Ferguson analysis. J Phys Chem. 2008; 112:7611–7676.
28. Pluen A, Boucher Y, Ramanujan S, McKee TD, Gohongi T, di Tomaso E, Brown EB, Izumi Y, Campbell RB, Berk DA, Jain RK. Role of tumor-host interactions in interstitial diffusion of macromolecules: cranial vs. subcutaneous tumors. Proc Natl Acad Sci USA. 2001; 98:4628–4633. [PubMed: 11274375]
29. Popovic Z, Liu W, Chauhan VP, Lee J, Wong C, Greytak AB, Insin N, Nocera DG, Fukumura D, Jain RK, Bawendi MG. A nanoparticle size series for in vivo fluorescence imaging. Angew Chem Int Ed Engl. 2010; 49:8649–8652. [PubMed: 20886481]
30. Ruoslahti E, Bhatia SN, Sailor MJ. Targeting of drugs and nanoparticles to tumors. J Cell Biol. 2010; 188:759– 768. [PubMed: 20231381]
31. Sarin H. Physiologic upper limits of pore size of different blood capillary types and another perspective on the dual pore theory of microvascular permeability. J Angiogenes Res. 2010; 2:14. [PubMed: 20701757]
32. Schmitt-Sody M, Strieth S, Krasnici S, Sauer B, Schulze B, Teifel M, Michaelis U, Naujoks K, Dellian M. Neovascular targeting therapy: paclitaxel encapsulated in cationic liposomes improves antitumoral efficacy. Clin Cancer Res. 2003; 9:2335–2341. [PubMed: 12796403]
33. Sevick EM, Jain RK. Viscous resistance to blood flow in solid tumors: effect of hematocrit on intratumor blood viscosity. Cancer Res. 1989; 49:3513–3519. [PubMed: 2731173]
34. Smith FG, Deen WM. Electrostatic effects on the partitioning of spherical colloids between dilute bulk solution and cylindrical pores. J Colloid Interface Sci. 1983; 91:571–590.
35. Stohrer M, Boucher Y, Stangassinger M, Jain RK. Oncotic pressure in solid tumors is elevated. Cancer Res. 2000; 60:4251–4255. [PubMed: 10945638]
36. Stylianopoulos T, Poh MZ, Insin N, Bawendi MG, Fukumura D, Munn LL, Jain RK. Diffusion of particles in the extracellular matrix: the effect of repulsive electrostatic interactions. Biophys J. 2010; 99:1342–1349. [PubMed: 20816045]
37. Stylianopoulos T, Yeckel A, Derby JJ, Luo XJ, Shephard MS, Sander EA, Barocas VH. Permeability calculations in three-dimensional isotropic and oriented fiber networks. Phys Fluids (1994). 2008; 20:123601. [PubMed: 19547721]
38. Sugahara KN, Teesalu T, Karmali PP, Kotamraju VR, Agemy L, Girard OM, Hanahan D, Mattrey RF, Ruoslahti E. Tissue-penetrating delivery of compounds and nanoparticles into tumors. Cancer Cell. 2009; 16:510–520. [PubMed: 19962669]
39. Tong RT, Boucher Y, Kozin SV, Winkler F, Hicklin DJ, Jain RK. Vascular normalization by vascular endothelial growth factor receptor 2 blockade induces a pressure gradient across the vasculature and improves drug penetration in tumors. Cancer Res. 2004; 64:3731–3736. [PubMed: 15172975]
40. Torchilin VP. Targeted pharmaceutical nanocarriers for cancer therapy and imaging. AAPS J. 2007; 9:E128–E147. [PubMed: 17614355]
41. Wong C, Stylianopoulos T, Cui J, Martin J, Chauhan VP, Jiang W, Popovic Z, Jain RK, Bawendi MG, Fukumura D. Multistage nanoparticle delivery system for deep penetration into tumor tissue. Proc Natl Acad Sci USA. 2011; 108:2426–2431. [PubMed: 21245339]
42. Wu J, Xu S, Long Q, Collins MW, Konig CS, Zhao G, Jiang Y, Padhani AR. Coupled modeling of blood perfusion in intravascular, interstitial spaces in tumor microvasculature. J Biomech. 2008; 41:996–1004. [PubMed: 18222455]
43. Yuan F, Dellian M, Fukumura D, Leunig M, Berk DA, Torchilin VP, Jain RK. Vascular permeability in a human tumor xenograft: molecular size dependence and cutoff size. Cancer Res. 1995; 55:3752–3756. [PubMed: 7641188]

44. Yuan F, Leunig M, Huang SK, Berk DA, Papahadjopoulos D, Jain RK. Microvascular permeability and interstitial penetration of sterically stabilized (stealth) liposomes in a human tumor xenograft. Cancer Res. 1994; 54:3352–3356. [PubMed: 8012948]

45. Yuan F, Salehi HA, Boucher Y, Vasthare US, Tuma RF, Jain RK. Vascular permeability and micro-circulation of gliomas and mammary carcinomas transplanted in rat and mouse cranial windows. Cancer Res. 1994; 54:4564–4568. [PubMed: 8062241]

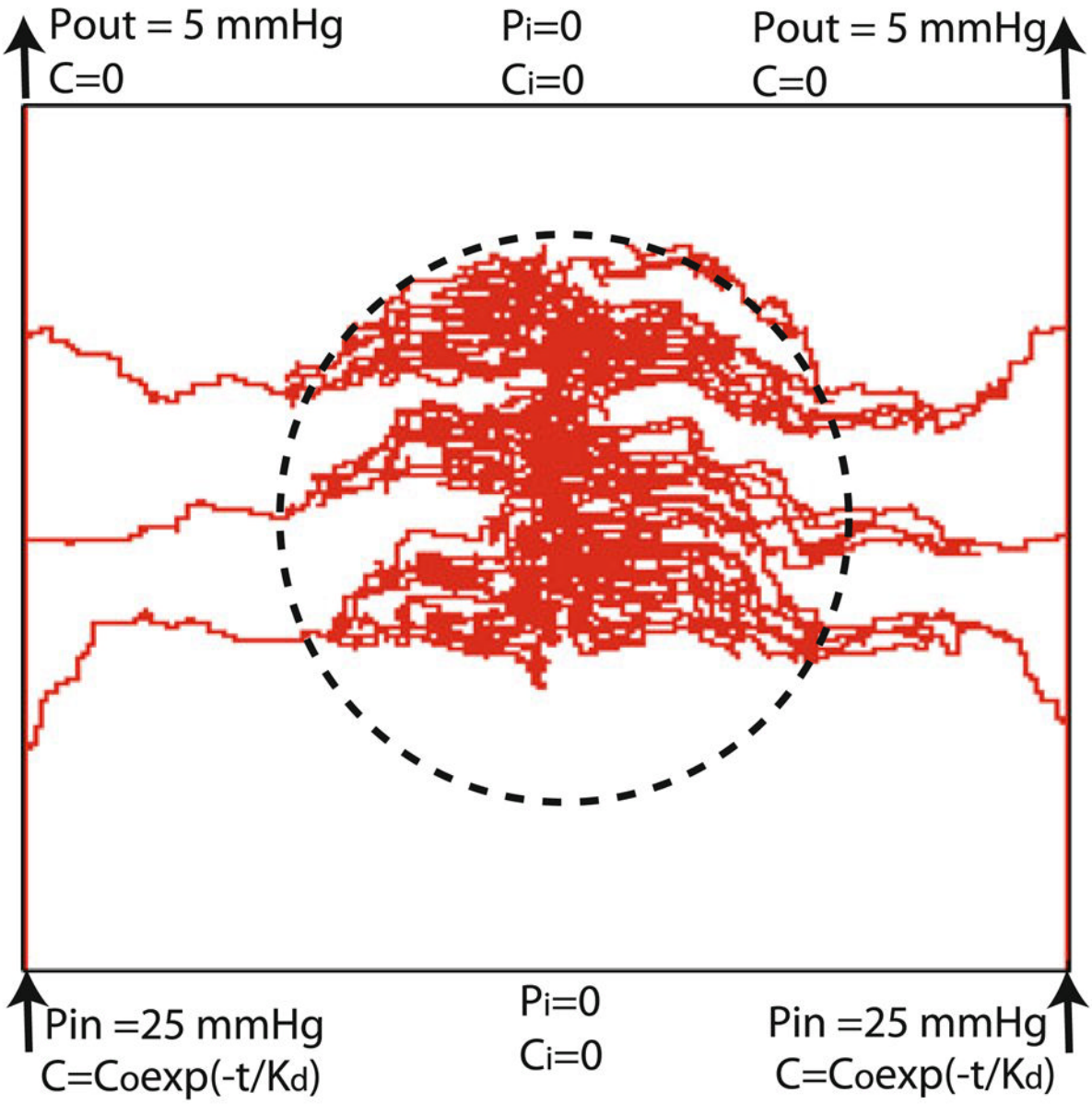

FIGURE 1.

Computational domain and boundary conditions employed in the study. The diameter of the tumor (shown with a dashed line) is 1 cm and the size of the whole domain is 2 × 2 cm. The vascular network consists of two parent vessels located at the two sides of the domain. Each parent vessel gives birth to three neoplastic vessels that branch as they move towards the tumor.

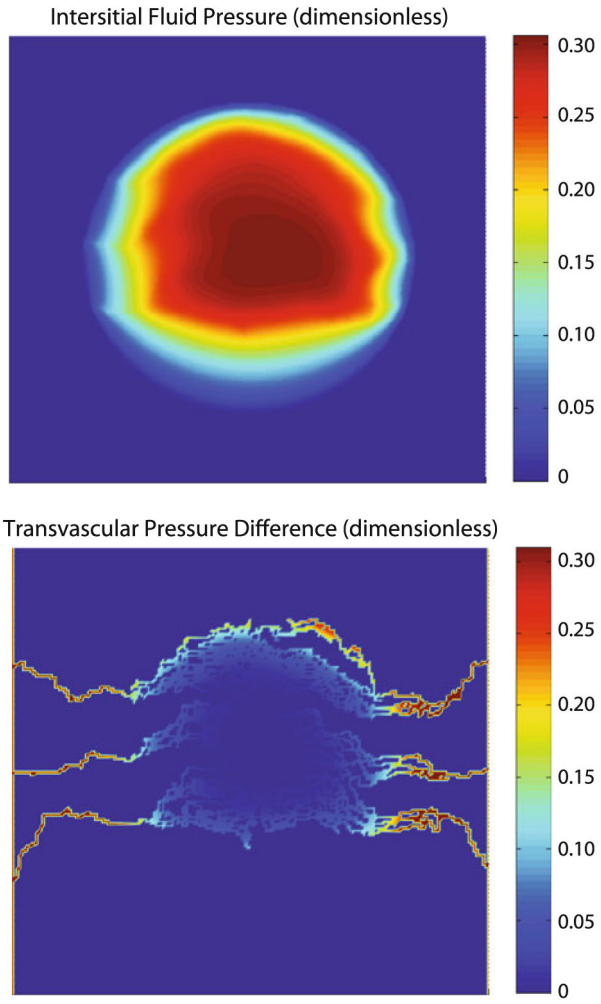

FIGURE 2.
Interstitial fluid pressure and transvascular pressure difference for the model parameters employed in the study. The mean pore size is 400 nm and the standard deviation 60 nm. Pressure values are made dimensionless by division with the vascular pressure at the inlet.

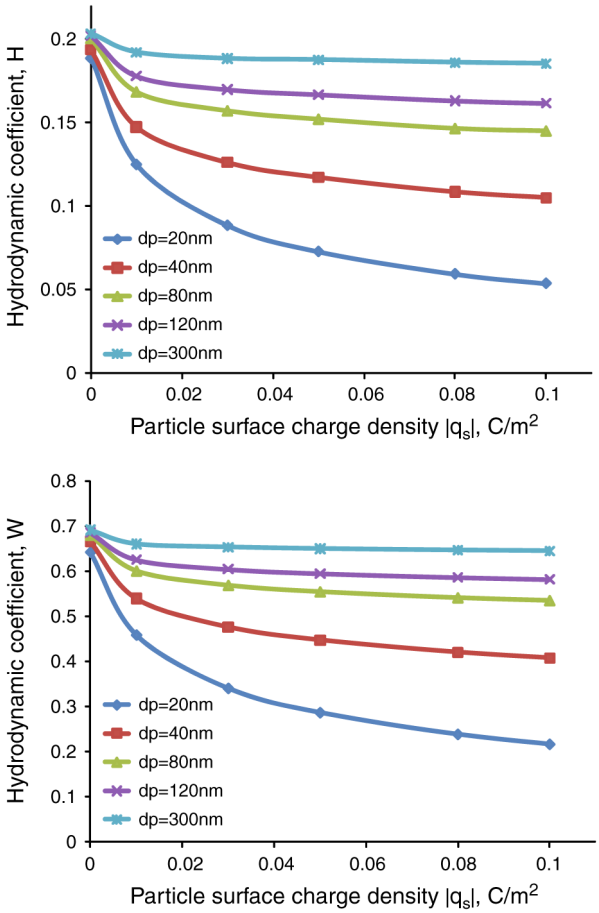

FIGURE 3.

Model predictions for the hydrodynamic coefficients H and W as a function of the surface charge density of negatively-charged particles for different values of pore sizes, d_p. The ratio of the particle size to pore size, λ, is 0.3 and the ionic strength is 0.15 M.

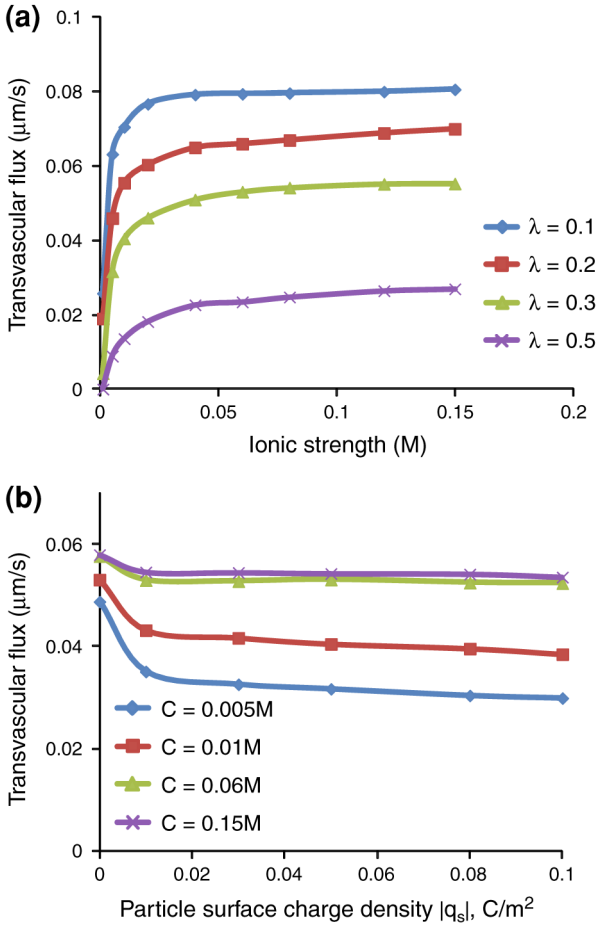

FIGURE 4.

Model predictions for the (a) transvascular flux as a function of the ionic strength for negatively-charged nanoparticles (q_s = −0.05 C/m^2) of four different sizes, λ = 0.1, 0.2, 0.3, and 0.5. (b) Transvascular flux as a function of the surface charge density for λ = 0.3 and ionic strength C = 0.005, 0.01, 0.06, and 0.15 M. The mean pore size was 400 nm with a standard deviation of 60 nm.

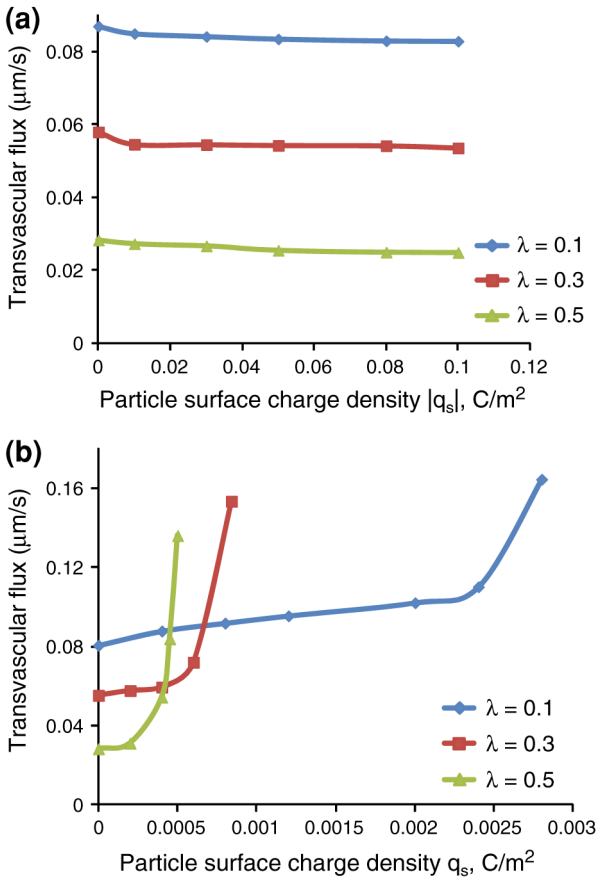

FIGURE 5.

Model predictions for the (a) transvascular flux as a function of surface charge density for negatively-charged particles with sizes $\lambda = 0.1$, 0.3, and 0.5. (b) Transvascular flux as a function of surface charge density for positively-charged particles with sizes $\lambda = 0.1$, 0.3, and 0.5. The mean pore size was 400 nm with a standard deviation of 60 nm.

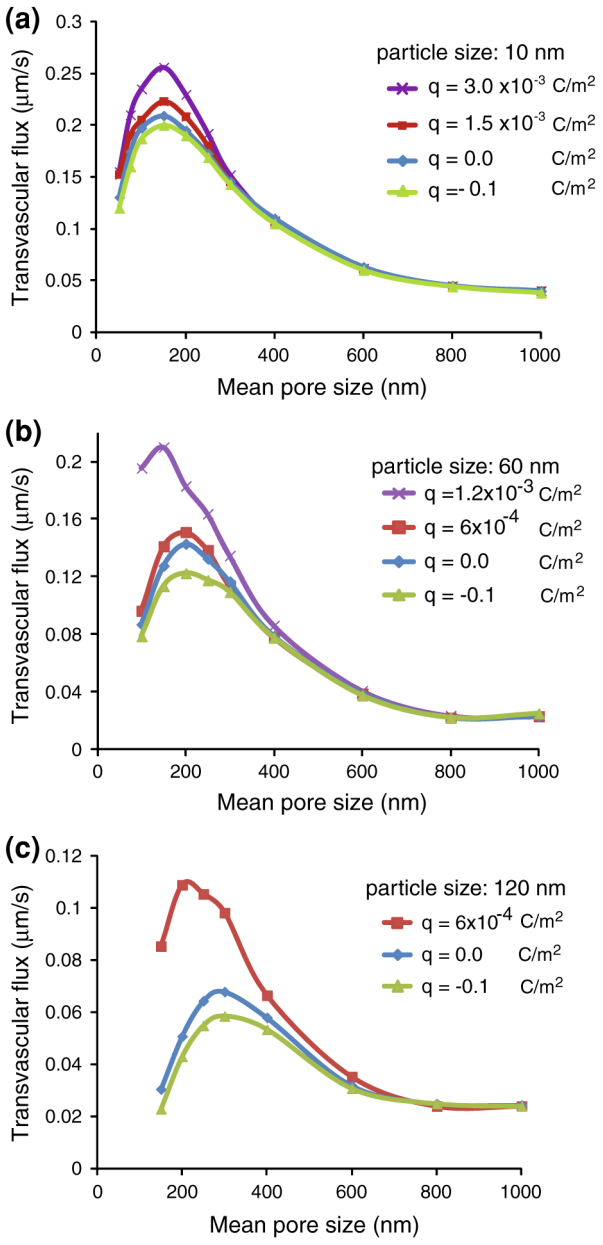

FIGURE 6.

Model predictions for the transvascular flux of 10 nm (a), 60 nm (b), and 120 nm (c) particles as a function of the mean pore size and for negatively-charged, neutral and positively-charged particles. Pore size standard deviation is 60 nm.

TABLE 1

Physiological parameter values.

Model parameters	Value	References
Vessel wall pore size	400 ± 60 nm	8,16
Vessel wall charge density	−0.05 C/m^2	34
Blood viscosity	3×10^{-5} mmHg s	19
Vascular pressure at the inlets	25 mmHg	3
Vascular pressure at the outlets	5 mmHg	3
Vascular density	100 cm^{-1}	44
Vessel wall thickness	5 μm	18
Vessel diameter	15 μm	45
Interstitial space conductivity	8×10^{-7} cm^2/mmHg s	25